Separation Science and Technology
Publication details, including instructions for authors and subscription information:
http://www.informaworld.com/smpp/title~content=t713708471

Morphology and Size of Cycloolefin Copolymer Precipitated from Toluene Solution Using Compressed CO_2 as Antisolvent

He-An Fan[a]; Chung-Sung Tan[a]
[a] Department of Chemical Engineering, National Tsing Hua University, Hsinchu, Taiwan, ROC

Online publication date: 08 July 2010

To cite this Article Fan, He-An and Tan, Chung-Sung(2005) 'Morphology and Size of Cycloolefin Copolymer Precipitated from Toluene Solution Using Compressed CO_2 as Antisolvent', Separation Science and Technology, 39: 15, 3453 — 3469
To link to this Article: DOI: 10.1081/SS-200028906
URL: http://dx.doi.org/10.1081/SS-200028906

SEPARATION SCIENCE AND TECHNOLOGY
Vol. 39, No. 15, pp. 3453–3469, 2004

Morphology and Size of Cycloolefin Copolymer Precipitated from Toluene Solution Using Compressed CO_2 as Antisolvent

He-An Fan and Chung-Sung Tan*

Department of Chemical Engineering, National Tsing Hua University, Hsinchu, Taiwan, ROC

ABSTRACT

The compressed CO_2 was observed to be an effective antisolvent to separate cycloolefin copolymer (COC) from toluene solution. The precipitation was carried out by spraying a toluene solution containing COC into a compressed CO_2 environment. It was found that more than 95% of the dissolved COC could be precipitated at the conditions that both gas and liquid CO_2 phases were present and the liquid level was located at the middle in the precipitator. Submicron-sized spheres of COC with a narrow size distribution were exhibited for the COC concentrations less than 6 wt%. The precipitation at these concentrations followed a nucleation and growth mechanism. Nucleation and solution

*Correspondence: Chung-Sung Tan, Department of Chemical Engineering, National Tsing Hua University, Hsinchu 300, Taiwan, ROC; Fax: 886-3-5721684; E-mail: cstan@che.nthu.edu.tw.

DOI: 10.1081/SS-200028906 0149-6395 (Print); 1520-5754 (Online)

breakup that affected morphology and size of the precipitated COC were allowed to occur in the gas space above the liquid. For the concentrations equal to and higher than 7 wt%, continuously interpenetrating structures instead of spheres and a decrease in porosity of the precipitated COC with increasing the COC concentration were exhibited, indicating the precipitation under a spinodal decomposition mechanism. The molecular weight and glass transition temperature of the precipitated COC were found to be sufficiently close to those of the virgin chips.

Key Words: Compressed carbon dioxide; Antisolvent; Cycloolefin; Copolymer; Morphology; Yield.

INTRODUCTION

Cycloolefin copolymer has been widely used as an optical wave-guided polymer. To precipitate COC from solution after synthesis, liquid antisolvents such as acetone and ketone are commonly used.[1,2] In these processes a complete removal of liquid antisolvent from the precipitated COC is generally difficult.

The recent reviews[3,4] have shown that compressed CO_2 is an effective antisolvent to precipitate polymers from organic solutions. With this operation, CO_2 can be easily removed from polymer after precipitation, and the operation variables including temperature, pressure, solute concentration, and injection rate can be easily adjusted to result in the desired morphology and size of the precipitated polymer.

When the compressed 1,1,1,2-tetrafluoroethane (HFC-134a) was used as the antisolvent, it was observed that submicron spheres of polystyrene and COC with a narrow size distribution could be precipitated from toluene solution at much lower pressures compared with that of CO_2.[5–7] Though HFC-134a has been proved to be an effective antisolvent, it may be prohibited for use in the future according to the Kyoto protocol. The objective of this study is therefore to use the compressed CO_2 as an antisolvent to generate spherically submicron-sized COC from a toluene solution. The operation variables, including temperature, pressure, COC concentration, flow rates of toluene and CO_2 were varied to see their effects on yield as well as the morphology and size of the precipitated COC. The mechanisms for the precipitation were also proposed.

EXPERIMENTAL

The experimental apparatus used for a continuous precipitation of COC from toluene solution using CO_2 as antisolvent is illustrated in Fig. 1.

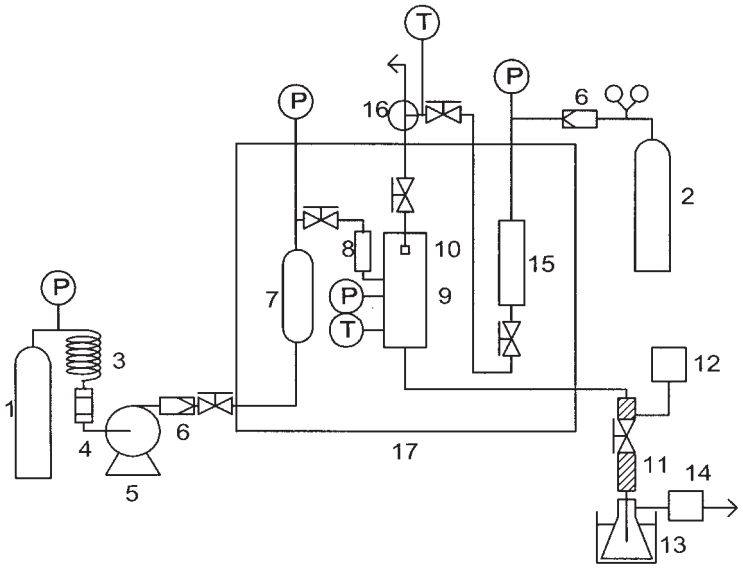

1. CO_2 cylinder
2. N_2 cylinder
3. Cooler
4. Filter
5. Pump
6. Check valve
7. Surge tank
8. Dehumidifier
9. Precipitator
10. Nozzle
11. Heating tape
12. Temperature controller
13. Cold trap
14. Wet gas meter
15. Jerguson gauge
16. Three-way valve
17. Constant temperature oven

P: Pressure indicator
T: Temperature indicator

Figure 1. Experimental apparatus for precipitation of COC using CO_2 as an antisolvent.

The precipitator was made of 316 stainless steel and had an inside diameter of 5 cm and a total volume of approximately 600 mL. It was equipped with two sapphire windows through which the precipitation of COC could be visualized. To trap the precipitated COC, a filter paper with a pore size of 0.45 μm (Millipore, HVHP04700) sitting on a 100-mesh stainless steel was placed at the bottom of the precipitator. The precipitator was placed in a constant temperature oven where the temperature could be maintained to within 0.2 K in a range of 253–333 K.

During the operation, CO_2 with a purity of 99.99% (SanFu Gas Co., Taiwan) was compressed by a minipump (Milton-Roy, NSI-33R) and was delivered to the top of the precipitator. The pressure inside the precipitator was read by a digital pressure indicator (Asahi, K054909). The flow rate

of CO_2 was measured by a wet gas meter (Shinagawa, W-NK-1) located downstream of the precipitator. A total of 20 g of solution containing 3–10 wt% COC was loaded into a 70 mL container (Jerguson Gauge, 13R-20) from which the amount of solution flowed into the precipitator could be read via sight glasses. The COC-toluene solution was prepared by dissolving a known amount of COC (Ticona, $T_g = 403$ K, $M_W = 1.04 \times 10^5$, and $M_W/Mn = 1.59$) in toluene (Mallinckrodt Baker Inc., 99.9% of purity).

The compressed nitrogen with 11 MPa was introduced instantaneously into the solution tank to deliver the toluene solution. In the preliminary runs, the amount of nitrogen dissolved in toluene was measured at the conditions without the presence of the compressed CO_2 in the precipitator. Almost no nitrogen was collected after the expansion of toluene in the precipitator when the compressed nitrogen was introduced into the solution tank right before the spray. Under this situation, nitrogen was believed to have a negligible effect on precipitation. After the desired temperature and pressure in the precipitator were reached, the COC-toluene solution was allowed to enter the precipitator through a hollow cone nozzle with a diameter of 0.4 mm and a length of 49.6 mm (Spraying System, TN-SS40). The flow rate of the toluene solution was adjusted with a metering valve (Whitey, SS-21RS2). The solution drained from the precipitator was collected in a cold trap where the temperature was maintained at 263 K. During the spray of the toluene solution, the pressure was observed to vary within ± 0.02 MPa.

After finishing the spray of the toluene solution, the compressed CO_2 continuously flowed though the precipitator for 1 h to remove toluene adhering to the precipitated COC trapped on the filter paper. After this extraction process, the pressure in the precipitator was reduced to atmosphere and the COC on the filter paper was collected. A known amount of toluene was then used to flush the precipitator in order to collect the residual COC deposited on the wall of the precipitator. COC in the drainage solution and in the flushing toluene solution were precipitated by adding three times the volume of acetone (Tedia Company Inc., 99.97% of purity) to the solutions. All the collected COC were heated in a vacuum at 353 K for 8 h before analysis. The collected COC from the filter paper and from the drainage and flushing solutions were weighed to check the overall mass balance.

The molecular weights and the glass transition temperatures (T_g) of the collected COC were determined by a gel permeation chromatograph (Shimazu, LC-9A) using THF as a mobile phase and a differential scanning calorimeter (TA Instruments, DSC 2920), respectively. Scanning electron microscopy (JEOL, JSM-5000) was used to examine the morphology of the collected COC.

RESULTS AND DISCUSSION

In each run, the injected amount of COC was compared to the overall mass of COC collected from the filter paper, the drainage solution, and the flushing solution. It was observed that these two masses were sufficiently close. The difference was always less than 2.0% for the runs resulting in microspheres of COC. In the mass balance calculation, the amounts of COC in the drainage and flushing solutions were found to be much smaller than that collected in the precipitator. The yield of COC was therefore defined as the fraction of the injected COC collected in the precipitator. It is also noted here that the morphology of the COC precipitated from the drainage and flushing solutions using acetone as antisolvent was completely different from that of the COC collected in the precipitator. The reproducibility tests were also performed at different temperatures, pressures, and flow rates of CO_2 and the toluene solution. The difference in yield was found to be always less than 3%. In addition to yield, the morphology and size of the collected COC in the precipitator were observed to be almost the same.

From Table 1 and Figs. 2 and 3, it can be seen that almost all the injected COC could be precipitated in the precipitator at any pressures but the morphologies of the precipitated COC were dependent on temperatures and pressures. The adsorption and desorption of krypton were measured volumetrically using ASAP 2010 analyzer (Micromeritics Co.) for the cases in which microspheres were generated. The adsorption isotherm data indicated that the generated microspheres were nonporous. When the pressure was below the vapor pressure of CO_2 at 25°C, embryos and fibers with few microspheres of the precipitated COC were exhibited. It is known that the volume expansion increases with increasing pressure. Under this situation, the supersaturation ratios at these pressures were not high enough to generate enough nuclei, and the growth of COC then became dominant and resulted in bulks of the precipitated COC. For the COC concentration of 3 wt%, less bulky structures were formed compared with that at 5 wt%. This was due to less COC that could be precipitated. When the pressure was raised to 6.41 MPa, which is the vapor pressure of CO_2 at 25°C, and the liquid CO_2 level was maintained at the middle of the precipitator, the precipitation was visualized when the solution hit liquid CO_2. Almost all the collected COC was exhibited as dispersed microspheres, similar to that using HFC-134a as the antisolvent.[7] The possible reason for the formation of microsphere was that the nucleation resulting from a high-volume expansion mainly occurred in the gas phase and the growth mainly happened in liquid phase. When the pressures were higher than the vapor pressure, the toluene solution jets were mixed with liquid CO_2 right after it flowed out of the nozzle. Though the supersaturation ratios were high enough to generate a large number of nuclei, the growth in the mixture of

Table 1. Effect of pressure on yield and morphology for the operations at a temperature of 25°C, a CO_2 flow rate of 2000 mL/min, and a toluene solution flow rate of 50 mL/min.

P MPa	ρ_{CO_2} g/cm^3	COC wt%	Yield* wt%	Macrostructure	Morphology and size
9.65	0.811	5	98.7	Fluffy powders	Submicron interconnected networks
8.27	0.78	5	97.2	Fluffy powders	Submicron interconnected networks
6.89	0.724	5	98.1	Fluffy powders	Submicron interconnected networks
6.41**	0.714(L) 0.241(V)	5	95.3	Sl. flocc./agglom. powders	Microspheres, 0.1–0.4 μm
6.20	0.23	5	96.4	Bulks	Microspheres and embryos
8.27	0.78	3	95.2	Fluffy powders	Submicron interconnected networks
6.41**	0.714(L) 0.241(V)	3	97.9	Sl. flocc./agglom. powders	Microspheres, 0.2–0.5 μm
6.20	0.23	3	97.5	Bulks	Microspheres and fibers

*Yield was defined as the ratio of the precipitated COC to the injected amount.
**The liquid CO_2 level was in the middle of the precipitator.

liquid CO_2 and toluene solution also happened. As a consequence, submicron interconnected networks were exhibited.

For the operations under the vapor pressures of CO_2 at temperatures lower than 25°C and the liquid CO_2 level at the middle of the precipitator, the morphology and size of the precipitated COC were nearly identical to those at 25°C, shown in Table 2 and Fig. 4. But when the temperature was higher than 25°C, for example, at 29°C, larger spheres with severe agglomeration were observed. Dixon et al.[8] observed that the precipitated PS was agglomerated severely at high operating temperatures using the compressed CO_2 as an antisolvent. They attributed this to the depression of the T_g of PS. Krause et al.[9] pointed out that the compressed CO_2 would depress the T_g of COC as well when it was used to form voids in a COC membrane. Based on these observations, it was believed that the severe agglomeration

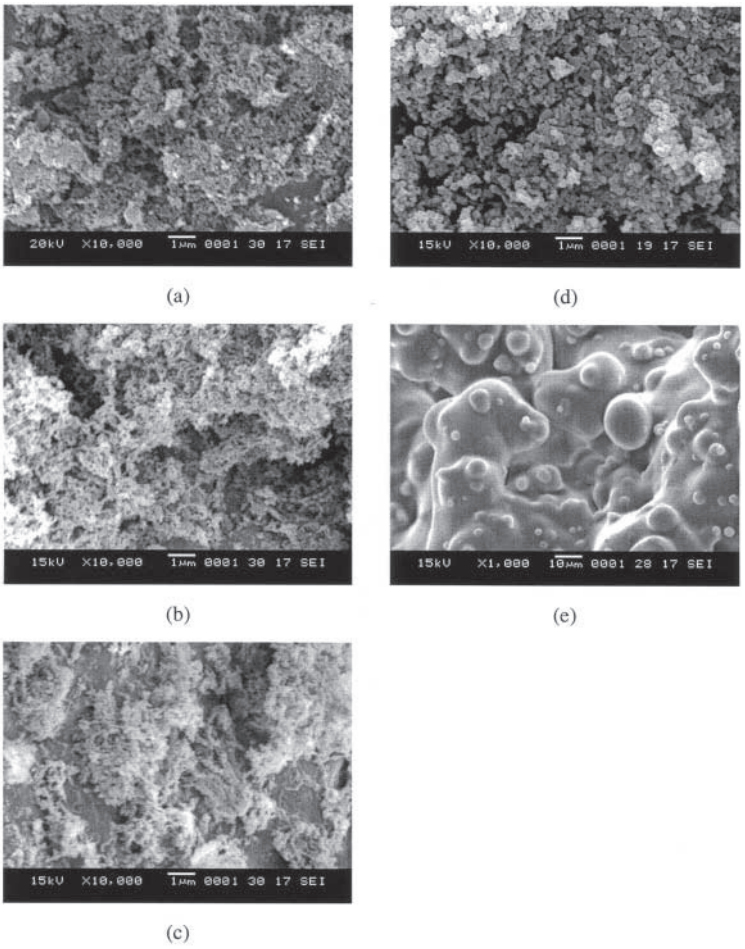

Figure 2. SEM of the precipitated COC by spraying a 5 wt% COC solution into CO_2 at a temperature of 25°C, a toluene solution flow rate of 50 mL/min, a CO_2 flow rate of 2000 mL/min, and the pressures of (a) 9.65 MPa, (b) 8.27 MPa, (c) 6.89 MPa, (d) 6.41 MPa, (e) 6.20 MPa.

of the precipitated COC at 29°C was due to a close of the operating temperature to the depressed T_g of COC.

With the operations with the use of supercritical CO_2 as an antisolvent, the precipitated COC exhibited more agglomeration compared to the operations with the coexistence of gas and liquid phases in the precipitator, shown in Table 3 and Fig. 5. It was also seen that agglomeration became

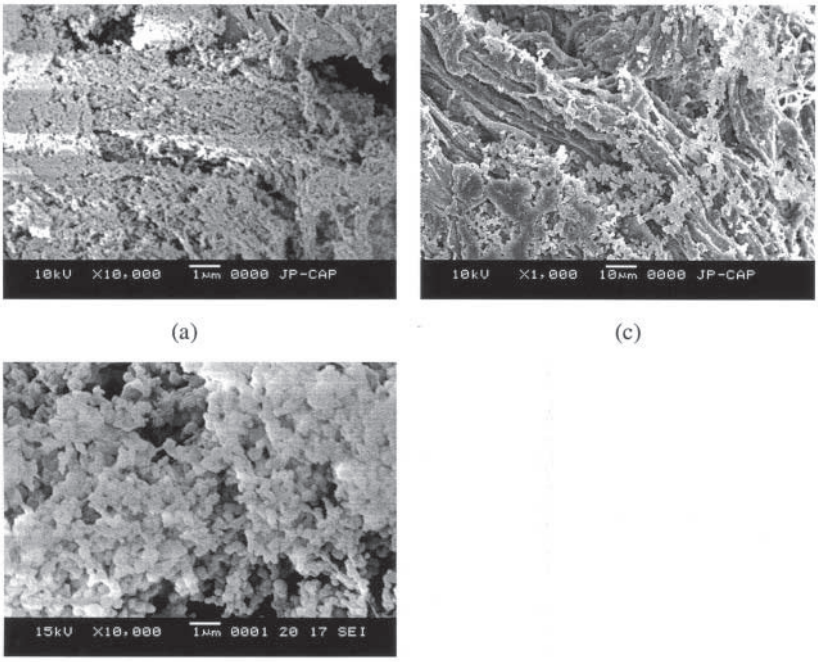

Figure 3. SEM of the precipitated COC by spraying a 3 wt% COC solution into CO_2 at a temperature of 25°C, a toluene solution flow rate of 50 mL/min, a CO_2 flow rate of 2000 mL/min, and the pressures of (a) 8.27 MPa, (b) 6.41 MPa, (c) 6.20 MPa.

more severe at higher-temperature operations, resulting from being closer to the depressed T_g. Under this situation, the macrostructures generated at supercritical conditions were exhibited as bulks rather than powders at 45°C. Because microspherical COC could not be generated, the precipitation using supercritical CO_2 as the antisolvent was not recommended.

Table 4 and Fig. 6 show the effects of the COC concentration on morphology of the precipitated COC when the CO_2 liquid level was kept at the middle in the precipitator. When the COC concentration was lower than 6 wt%, the precipitated COC were exhibited as microspheres. Because the morphology and size of the precipitated COC were similar to those of COC and polystyrene using HFC-134a and CO_2 as the antisolvent, respectively,[7,10] it was therefore anticipated that the present precipitation followed the nucleation and growth mechanism. When the concentration was equal to and larger than 7 wt%, a continuously interpenetrating structure with voids

Table 2. Effect of temperature on yield and morphology at a CO_2 flow rate of 2000 mL/min, a toluene solution flow rate of 50 mL/min, and a liquid CO_2 level in the middle of the precipitator.

T °C	P MPa	COC wt%	ρ_{co_2} g/cm^3	Yield wt%	Macrostructure	Morphology and size
25	6.41	5	0.714(L) 0.241(V)	95.3	Sl. flocc./agglom. powders	Microspheres, 0.1–0.4 μm
15	5.07	5	0.823(L) 0.16(V)	95.5	Sl. flocc./agglom. powders	Microspheres, 0.1–0.4 μm
5	3.96	5	0.897(L) 0.114(V)	98.1	Sl. flocc./agglom. powders	Microspheres, 0.1–0.4 μm
25	6.41	3	0.714(L) 0.241(V)	97.9	Sl. flocc./agglom. powders	Microspheres, 0.2 0.5 μm
15	5.07	3	0.823(L) 0.16(V)	96.5	Sl. flocc./agglom. powders	Microspheres, 0.2–0.5 μm

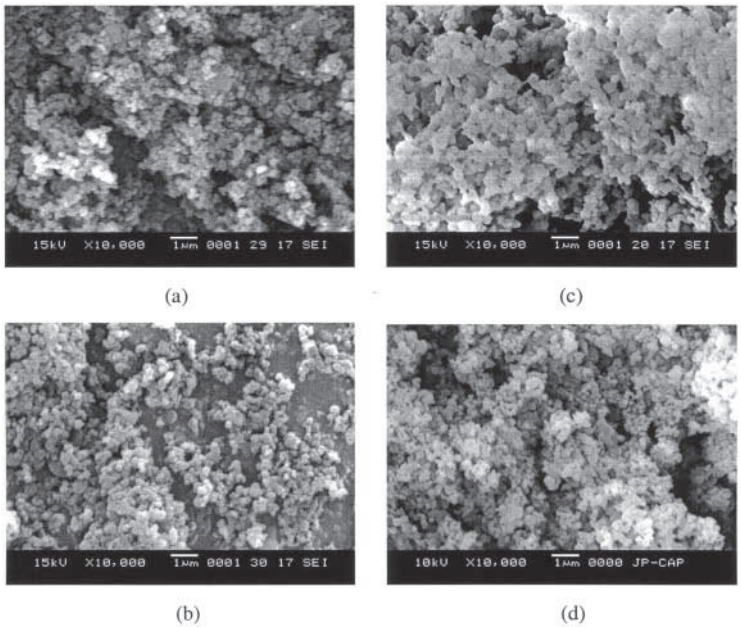

Figure 4. SEM of the precipitated COC at a toluene solution flow rate of 50 mL/min and a CO_2 flow rate of 2000 mL/min for the temperatures, pressures, and concentrations of (a) 15°C, 5.07 MPa, 5 wt%, (b) 5°C, 3.96 MPa, 5 wt%, (c) 25°C, 6.41 MPa, 3 wt%, (d) 15°C, 5.07 MPa, 3 wt%.

Table 3. Yield and morphology for the operations at supercritical conditions at a CO_2 flow rate of 2000 mL/min and a toluene solution flow rate of 50 mL/min.

T °C	P MPa	COC wt%	ρ_{CO_2} g/cm^3	Yield wt%	Macrostructure	Morphology and size
35	8.27	5	0.575	97.0	Sl. flocc/agglom. powders	Microspheres and coalescence of microparticles
35	9.65	5	0.613	97.8	Sl. flocc./agglom. powders	Microspheres and coalescence of microparticles
45	8.27	5	0.287	98.9	Airy-bulks	Foaming structures
45	9.65	5	0.458	97.0	Bulks	Coalescence of microparticles

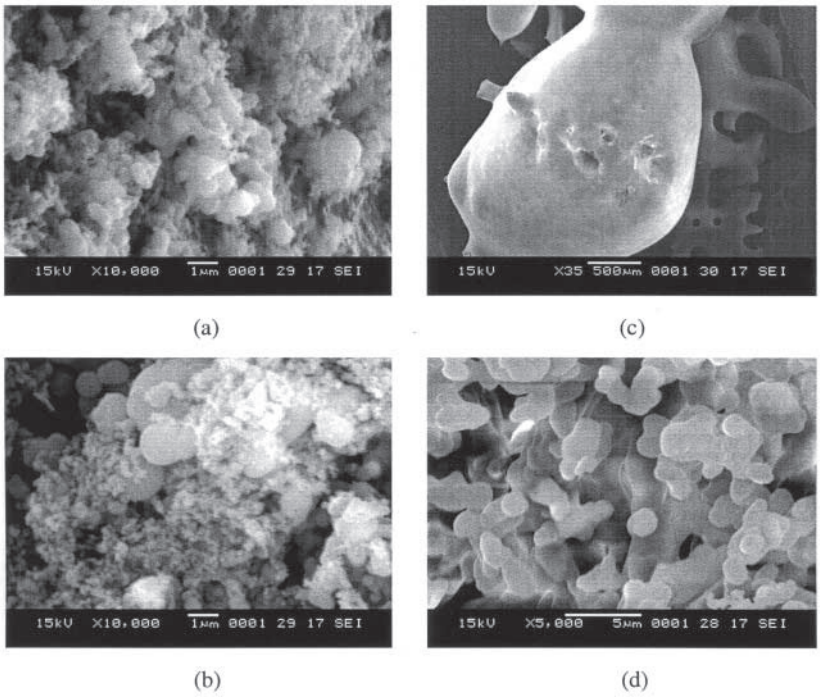

Figure 5. SEM of the precipitated COC at a COC concentration of 5 wt%, a toluene solution flow rate of 50 mL/min, and a CO_2 flow rate of 2000 mL/min for the temperatures and pressures of (a) 35°C, 8.27 MPa, (b) 35°C, 9.65 MPa, (c) 45°C, 8.27 MPa, (d) 45°C, 9.65 MPa.

Table 4. Effect of COC concentration on yield and morphology for the operations at a temperature of 25°C, a pressure of 6.41 MPa, a CO_2 flow rate of 2000 mL/min, a toluene solution flow rate of 50 mL/min, and a liquid CO_2 level in the middle of the precipitator.

COC wt%	ρ_{CO_2} g/cm^3	Yield wt%	Macrostructure	Morphology and size
3	0.714(L) 0.241(V)	97.9	Sl. flocc./agglom. powders	Microspheres, 0.2–0.5 μm
5	0.714(L) 0.241(V)	95.3	Sl. flocc./agglom. powders	Microspheres, 0.1–0.4 μm
6	0.714(L) 0.241(V)	96.5	Sl. flocc./agglom. powders	Microspheres and coalescence of microparticles
7	0.714(L) 0.241(V)	99.6	Bulks	Continuously interpenetrating structures
8	0.714(L) 0.241(V)	98.7	Bulks	Continuously interpenetrating structures
10	0.714(L) 0.241(V)	96.8	Bulks	Continuously interpenetrating structures

rather than microsphere was generated, shown in Fig. 6. It is also seen from Fig. 6 that a more continuous structure was formed and the porosity of the precipitated COC was decreased when the COC concentration was increased, just as for that using HFC-134a as an antisolvent.[7] These observations indicated that more vitrification occurred at higher polymer concentrations.[7,10] Based on these observations, it was concluded that the precipitation followed a spinodal decomposition in which a spontaneous phase separation occurred in the gas space.

Beside the precipitation mechanisms, the variation in morphology with concentration was also affected by the stabilization of the solution jet. The viscosity of the 8 wt% solution was estimated to be about twice that of the 5 wt% solution, but the densities of these two solutions were not a significant difference. Because the CO_2 and solution flow rates were the same for these two concentrations, the Reynolds number of the 8 wt% solution was calculated to be about half of that of the 5 wt% solution. In addition to the Reynolds number, the Weber number was also believed to decrease for a higher COC concentration due to an increase in interfacial tension. The decrease in Reynolds and Weber numbers hence reduced the jet breakup.[7,11] Besides, the entanglement between polymer

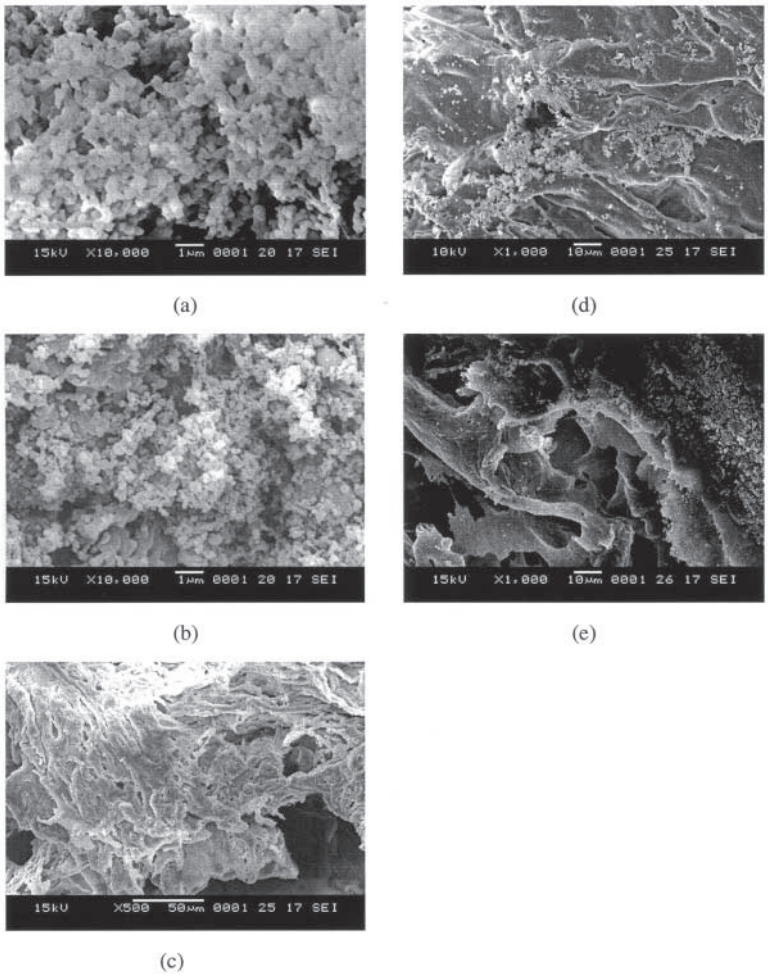

Figure 6. SEM of the precipitated COC at a toluene solution flow rate of 50 mL/min and a CO_2 flow rate of 2000 mL/min for the concentrations of (a) 3 wt%, (b) 6 wt%, (c) 7 wt%, (d) 8 wt%, (e) 10 wt%.

chains in a high-polymer concentration solution would obviously stabilize the liquid jet. These effects were more pronounced for the COC concentrations higher than 8 wt%. Under these circumstances, the spherical shape of the precipitated COC could not be generated.

As shown in Table 5, the morphology and size of the precipitated COC were found to be unchanged at different CO_2 flow rates when the

Table 5. Effect of CO_2 flow rate on yield and morphology for the operations at a temperature of 25°C, a pressure of 6.41 MPa, a toluene solution flow rate of 50 mL/min, and a liquid CO_2 level in the middle of the precipitator.

COC wt%	Q_{CO_2} mL/min	ρ_{CO_2} g/cm^3	Yield wt%	Macrostructure	Morphology and size
5	1,000	0.714(L) 0.241(V)	95.6	Sl. flocc./agglom. powders	Microspheres, 0.1–0.4 μm
5	2,000	0.714(L) 0.241(V)	95.3	Sl. flocc./agglom. powders	Microspheres, 0.1–0.4 μm
5	4,000	0.714(L) 0.241(V)	98.1	Sl. flocc./agglom. powders	Microspheres, 0.1–0.4 μm
3	1,000	0.714(L) 0.241(V)	96.0	Sl. flocc./agglom. powders	Microspheres, 0.2–0.5 μm
3	2,000	0.714(L) 0.241(V)	97.9	Sl. flocc./agglom. powders	Microspheres, 0.2–0.5 μm
3	4,000	0.714(L) 0.241(V)	97.7	Sl. flocc./agglom. powders	Microspheres, 0.2–0.5 μm

COC concentrations were maintained as constant. The observed results for particle size were slightly different from that using HFC-134a as an antisolvent in which the particle sizes were observed to increase with increasing antisolvent flow rate, though not significantly.[7] Hsu et al.[7] and Mawson et al.[12] described the increase in particle size with increasing antisolvent flow rate in terms of Reynolds and Weber numbers. The invariant size for a fixed COC concentration at different CO_2 flow rates indicated that the Reynolds and Weber numbers were high enough to result in a satisfactory jet breakup and mass transfer between CO_2 and solution.

When the CO_2 flow rate was maintained at 2000 mL/min, Table 6 shows that microspheres could be formed when the flow rates of the toluene solution were at 50 and 100 mL/min. An increase in toluene solution flow rate benefited the breakup of the solution jet into fine droplets and yielded smaller particles as a result. This was the reason for the formation of smaller particles at 100 mL/min compared to 50 mL/min. When the concentration was of 3 wt%, smaller microspheres were exhibited compared with those of 5 wt%. This was due to the fact that the solution jet for the 3 wt% solution was easier to break up because it was a less viscous fluid compared to that for the 5 wt% solution.

When the gas and liquid CO_2 coexisted in the precipitator, the morphology and size of the precipitated COC at different liquid levels are shown in Table 7 and Fig. 7. It can be seen that microspheres were formed at the

Table 6. Effect of toluene solution flow rate on yield and morphology for the operations at a temperature of 25°C, a pressure of 6.41 MPa, and a liquid CO_2 level in the middle of the precipitator.

COC wt%	$Q_{solution}$ mL/min	ρ_{CO_2} g/cm^3	Yield wt%	Macrostructure	Morphology and size
5	50	0.714(L) 0.241(V)	97.0	Sl. flocc./agglom. powders	Microspheres, 0.1–0.4 μm
5	100	0.714(L) 0.241(V)	97.4	Sl. flocc./agglom. powders	Microspheres, 0.1–0.3 μm
3	50	0.714(L) 0.241(V)	97.9	Sl. flocc./agglom. powders	Microspheres, 0.2–0.5 μm
3	100	0.714(L) 0.241(V)	97.5	SI. flocc./agglom. powders	Microspheres, 0.1–0.3 μm

liquid levels of 1/2 and 1/4 of the precipitator but fibers and a coalescence of microparticles were formed at a liquid level of 3/4. Because the breakup of the solution jet and the nucleation both easily occurred in the gas phase due to low density, very low surface tension, and high inertial force of the gas, the space of the gas phase at the liquid levels of 1/2 and 1/4 was therefore large enough to result in fine droplets. Under this circumstance,

Table 7. Effect of the liquid CO_2 level on yield and morphology for the operations at temperature of 25°C and a pressure of 6.41 MPa.

COC wt%	Liquid level	ρ_{CO_2} g/cm^3	Yield wt%	Macrostructure	Morphology and size
5	3/4	0.714(L) 0.241(V)	99.9	Sl. flocc./agglom. powders	Expanded fibers
5	1/2	0.714(L) 0.241(V)	95.3	Sl. flocc./agglom. powders	Microspheres, 0.1–0.4 μm
5	1/4	0.714(L) 0.241(V)	96.4	Sl. flocc./agglom. powders	Microspheres, 0.1–0.4 μm
3	3/4	0.714(L) 0.241(V)	99.2	Sl. flocc./agglom. powders	Coalescence of microparticles
3	1/2	0.714(L) 0.241(V)	97.9	Sl. flocc./agglom. powders	Microspheres, 0.2–0.5 μm
3	1/4	0.714(L) 0.241(V)	98.4	Sl. flocc./agglom. powders	Microspheres, 0.2–0.5 μm

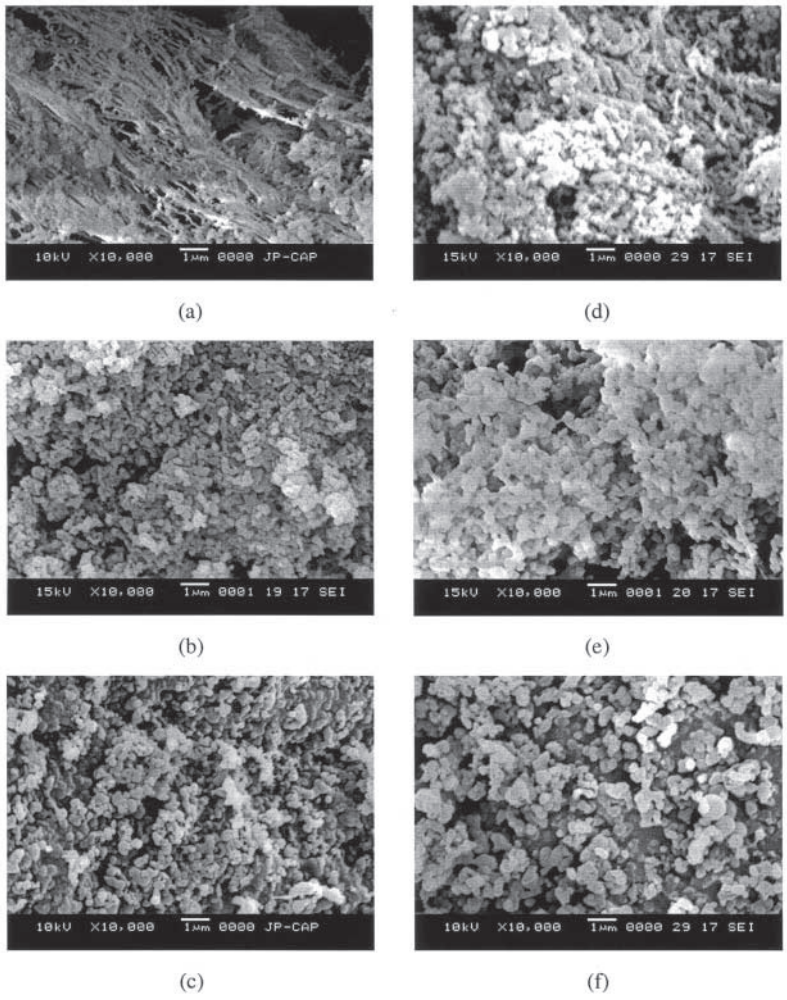

Figure 7. SEM of the precipitated COC at 25°C, 6.41 MPa, a toluene solution flow rate of 50 mL/min, and a CO_2 flow rate of 2000 mL/min for the liquid CO_2 levels and concentrations of (a) 3/4, 5 wt%, (b) 1/2, 5 wt%, (c) 1/4, 5 wt%, (d) 3/4, 3 wt%, (e) 1/2, 3 wt%, (f) 1/4, 3 wt%.

microspheres could be generated. When the liquid level was at 3/4 of the precipitator, the gas space was not large enough to form fine droplets. Consequently, fibers and a coalescence of microparticles instead of microspheres were formed.

The molecular weights and molecular weight distributions of the precipitated COC obtained at the operations in that both gas and liquid CO_2 existed and the liquid level was at the middle in the precipitator were found to be sufficiently close to those of the parent COC chips. The differences were found to be always less than 2.0%. Besides, the T_g was found to be nearly identical to that of the original chips (403 K). These results also indicated that toluene could be completely removed from the precipitated COC particles.

CONCLUSIONS

In a continuous spray of the COC-toluene solution into the compressed CO_2, almost all the dissolved COC could be precipitated from the solution when the precipitator was filled with liquid, gas, or both liquid and gas phases of CO_2. However, only microspherical COC could be precipitated at the operations in that both liquid and gas existed and the liquid level was at the middle in the precipitator. This kind of operation was therefore suggested. The molecular weight and its distribution as well as the glass transition temperature of the precipitated COC were found to be sufficiently close to those of the original COC chips as well, indicating that CO_2 was an appropriate antisolvent to separate COC from toluene.

The morphology of the precipitated COC was observed to be strongly dependent on the COC concentration. For the COC concentrations that were smaller than 6 wt%, submicron-sized spheres with a rather uniform size distribution could be generated. The precipitation at these concentrations was under a nucleation and growth mechanism. Nucleation mainly occurred in the gas space above the liquid CO_2. The gas space also allowed the solution to break up into fine droplets that affected the ultimate size of the precipitated COC. Because of the formation of fine powders consisting of slightly agglomerated microspheres, a high bulk density of the precipitated COC that is generally required for subsequent processing could then be obtained. But when the COC concentration was equal to or larger than 7 wt%, continuously interpenetrating structures instead of microspheres were exhibited. These morphologies partly resulted from a difficulty to break up a viscous solution jet. The precipitation at these concentrations followed a spinodal decomposition mechanism. The CO_2 flow rate did not affect morphology and size of the precipitated COC significantly, but smaller microspheres were exhibited at a higher toluene solution flow rate resulting from an enhancement of solution breakup. When the liquid level of CO_2 was raised from $1/2$ to $3/4$ of the precipitator, the gas space was found not to be enough to form fine droplets. As a result, microspheres could not be generated.

REFERENCES

1. Weller, T.; Brekner, M.J.; Osan, F. Process for Preparation and Purification of Material of a Cycloolefin Copolymer. US Patent 5,498,677, 1996.
2. Brekner, M.J.; Deckers, H.; Osan, F. Cycloolefin Copolymers Having Low Melt Viscosity and Low Optical Attenuation. US Patent 5,637,400, 1997.
3. Jung, J.; Perrut, M. Particle design using supercritical fluids: literature and patent survey. Supercri. Fluids **2001**, *20*, 179–219.
4. Reverchon, E. Supercritical antisolvent precipitation of micro- and nanoparticles. Supercri. Fluids **1999**, *15*, 1–21.
5. Tan, C.S.; Chang, W.W. Precipitation of polystyrene from toluene with HFC-134a by the GAS process. Ind. Eng. Chem. Res. **1998**, *37* (5), 1821–1826.
6. Tan, C.S.; Lin, H.Y. Precipitation of polystyrene by spraying polystyrene-toluene solution in to compressed HFC-134a. Ind. Eng. Chem. Res. **1999**, *38* (10), 3898–3902.
7. Hsu, R.Y.; Tan, C.S.; Chen, J.M. Formation of micron-sized cycloolefin copolymer from toluene solution using compressed HFC-134a as antisolvent. Appl. Polym. Sci. **2002**, *84*, 1657–1668.
8. Dixon, D.J.; Johnston, K.P.; Bodmeier, R.A. Polymeric materials formed by precipitation with a compressed fluid antisolvent. AIChE **1993**, *39*, 127–139.
9. Krause, B.; Mettinkhof, R.; van der Vget, N.F.A.; Wessling, M. Microcellular foaming of amorphous high-T_g polymers using carbon dioxide. Macromolecules **2001**, *34*, 874–884.
10. Dixon, D.J.; Luna-Bárcenas, G.; Johnston, K.P. Microcellular microspheres and microballoons by precipitation with a vapor-liquid compressed fluid antisolvent. Polymer **1994**, *35*, 3998–4005.
11. Lefebvre, A.H. *Atomization and Sprays*; Hemisphere: New York, 1989.
12. Mawson, S.; Kanakia, S.; Johnston, K.P. Coaxial nozzle for control of particle morphology in precipitation with a compressed fluid antisolvent. Appl. Polym. Sci. **1997**, *64*, 2105–2118.

Received September 2003
Accepted June 2004